Global particle simulation of lower hybrid wave propagation and mode conversion in tokamaks

J. Bao[1, 2, a)], Z. Lin[2] and A. Kuley[2, 1]

[1]*Fusion Simulation Center and State Key Laboratory of Nuclear Physics and Technology, Peking University, Beijing 100871, People's Republic of China*
[2] *Department of Physics and Astronomy, University of California, Irvine, CA 92697, USA*

[a)] Corresponding author: baojian@pku.edu.cn

Abstract. Particle-in-cell simulation of lower hybrid (LH) waves in core plasmas is presented with a realistic electron-to-ion mass ratio in toroidal geometry. Due to the fact that LH waves mainly interact with electrons to drive the current, ion dynamic is described by cold fluid equations for simplicity, while electron dynamic is described by drift kinetic equations. This model could be considered as a new method to study LH waves in tokamak plasmas, which has advantages in nonlinear simulations. The mode conversion between slow and fast waves is observed in the simulation when the accessibility condition is not satisfied, which is consistent with the theory. The poloidal spectrum upshift and broadening effects are observed during LH wave propagation in the toroidal geometry.

INTRODUCTION

Wentzel–Kramers–Brillouin (WKB) and full-wave approaches [1-4] have been widely used in studying the linear propagation and quasi-linear absorption of LH waves in tokamaks. However, there are still some unsolved problems for LH waves in fusion plasmas such as 'density limit' [5] and 'spectral gap' [6], which are considered to be related with nonlinear physics. For example, parametric decay instabilities of LH waves have been observed in some experiments [7-11]. Particle-in-cell (PIC) simulation approach is a powerful tool for studying the nonlinear physics of LH waves.

We use PIC approach to simulate LH waves by utilizing the existing physics capability, toroidal geometry and computational power of the gyrokinetic toroidal code (GTC) [12]. Thanks to the upgrade in previous works [13, 14], electromagnetic capability for the LH wave simulation has been developed in GTC to study mode conversion and propagation with the realistic parameters. In the current work, we find that launching from the high field side is helpful to LH wave penetration into the core plasma, which is associated with the poloidal spectrum upshift of the wave-packet. Furthermore, propagation and absorption of LH waves in hot plasmas are studied.

SIMULATION MODEL

To simulate LH waves with negligible damping from ion species, ion dynamic is described by cold fluid equations in canonical form as:

$$m_i n_{i0}\frac{d\boldsymbol{\delta}\mathbf{U_i}}{dt} = -Z_i n_{i0}\nabla\left[\phi - \frac{1}{c}\boldsymbol{\delta}\mathbf{u_i}\bullet\left(\mathbf{A_0}+\boldsymbol{\delta}\mathbf{A}\right)\right], \tag{1}$$

$$\boldsymbol{\delta}\mathbf{u_i} = \frac{1}{m_i}\left[\boldsymbol{\delta}\mathbf{U_i} - \frac{Z_i}{c}\left(\mathbf{A_0}+\boldsymbol{\delta}\mathbf{A}\right)\right], \tag{2}$$

Radio Frequency Power in Plasmas
AIP Conf. Proc. 1689, 080008-1–080008-4; doi: 10.1063/1.4936531

$$\frac{\partial \delta n_i}{\partial t} + n_{i0} \nabla \bullet \boldsymbol{\delta} \mathbf{u_i} = 0 , \tag{3}$$

where $\boldsymbol{\delta}\mathbf{U_i}$ and $\boldsymbol{\delta}\mathbf{u_i}$ are the canonical fluid velocity and mechanical fluid velocity, respectively. ϕ is the scalar potential, $\mathbf{A_0}$ is the equilibrium vector potential, and $\boldsymbol{\delta}\mathbf{A}$ is the perturbed vector potential.

Using canonical momentum $p_\parallel$, guiding center position $\mathbf{X}$ and magnetic momentum μ as independent variables in five dimensional phase space, drift kinetic equations for electron are[15,16]:

$$\frac{\partial f_e}{\partial t} + \dot{\mathbf{X}} \bullet \nabla f_e + \dot{p}_\parallel \frac{\partial f_e}{\partial p_\parallel} = 0 , \tag{4}$$

$$\dot{\mathbf{X}} = \left(p_\parallel - \frac{q_e}{c} \delta A_\parallel \right) \frac{\mathbf{B}_0^{*c}}{m_e B_0} + \frac{c \mathbf{b_0}}{q_e B_0} \times \left(\mu \nabla B_0 + q_e \nabla \Psi \right), \tag{5}$$

$$\dot{p}_\parallel = - \frac{\mathbf{B}_0^{*c}}{B_0} \bullet \left(\mu \nabla B_0 + q_e \nabla \Psi \right), \tag{6}$$

where $\mathbf{B_0} = B_0 \mathbf{b_0}$ is the equilibrium magnetic field, $\mathbf{B_0^{*c}} = \mathbf{B_0} + \frac{c}{q_e} p_\parallel \nabla \times \mathbf{b_0}$, $\delta B_\parallel$ and $\delta A_\parallel$ are the compressional magnetic field perturbation and the parallel vector potential, respectively. $p_\parallel = m_e v_\parallel + \frac{q_e}{c} \delta A_\parallel$, and $q_e \Psi = q_e \phi - q_e \frac{p_\parallel \delta A_\parallel}{m_e c} + \mu \delta B_\parallel + \frac{q_e^2 \delta A_\parallel^2}{2 m_e c^2}$ is the generalized potential.

Parallel Ampere's law is used for solving $\delta A_\parallel$ as:

$$\left(\nabla_\perp^2 - \frac{\omega_{pe}^2}{c^2} \right) \delta A_\parallel = - \frac{4\pi}{c} \left(J_{i\parallel} + J_{e\parallel} \right), \tag{7}$$

where $J_{i\parallel} = Z_i n_{i0} \delta u_{i\parallel}$ and $J_{e\parallel} = \frac{q_e}{m_e} \int \delta f_e p_\parallel \mathbf{dv}$, $\delta u_{i\parallel}$ is the parallel mechanical fluid velocity of ion. The second term on the LHS of Eq. (7) is due to the difference between $p_\parallel$ and $m_e v_\parallel$.

With assuming $\nabla \times \mathbf{B_0} = 0$ and f_0 is a Maxwellian, the Poisson's equation becomes [16,17]:

$$\nabla_\perp \bullet \left(1 + \frac{\omega_{pe}^2}{\Omega_{ce}^2} \right) \nabla_\perp \phi + \frac{4\pi n_e q_e}{B_0} \delta B_\parallel = -4\pi \left(Z_i \delta n_i + q_e \delta n_e \right) + 4\pi q_e \nabla \left(\frac{n_e}{B_0^2} \right) \bullet \mathbf{B} \times \boldsymbol{\delta} \mathbf{A}_\perp . \tag{8}$$

The last term on the LHS and the RHS of Eq. (8) are from the $\partial \mathbf{A}_\perp / \partial t$ induced electron $\mathbf{E} \times \mathbf{B}$ motion.

In LH wave frequency range $\omega \ll \Omega_{ce}$, we can apply electron perpendicular force balance equation as:

$$n_e q_e \boldsymbol{\delta} \mathbf{E}_\perp = \nabla_\perp \bullet \boldsymbol{\delta} \mathbf{P_e} - \frac{1}{c} \mathbf{J}_{e\perp} \times \mathbf{B}_0 . \tag{9}$$

Eqs. (1-9) form a closed system, which are used to investigate the linear electromagnetic properties of LH waves in tokamaks.

MODE CONVERSION

Mode conversion between slow wave and fast wave will happen if the local accessibility condition is not satisfied, namely, when the parallel refractive index of LH wave is smaller than the threshold: $n_{\|} < n_a$ [1]. Here, we will study LH wave mode conversion with different launch positions in the tokamak geometry.

In the simulation, the plasma is non-uniform with the on-axis value of the electron density $n_{i0} = n_{e0} = 2.0 \times 10^{14} cm^{-3}$, and the on-axis value of the magnetic field is $B_a = 5.0T$. The minor and major radii are $a = 0.16m$, $R_0 = 0.64m$, respectively. The LH wave frequency is $f_0 = 4.6GHz$ and the toroidal refractive index is $n_t = ck_t/\omega = 1.86$. We launch the slow wave at poloidal angle $\theta = 0$, $\theta = 0.125\pi$ and $\theta = 0.25\pi$, respectively, as shown in Figs. 1(a)-(c). The central poloidal mode number m_0 of the wave-packet is measured at different flux surfaces for these three cases. We find that moving the launch position from the low field side to the high field side can lead to a larger increase of m_0 as shown in Figs. 1(d)-(f), namely, a the larger increase of the parallel reflective index $n_{\|}$, which is helpful for the wave penetration into the core plasma and for avoiding the mode conversion.

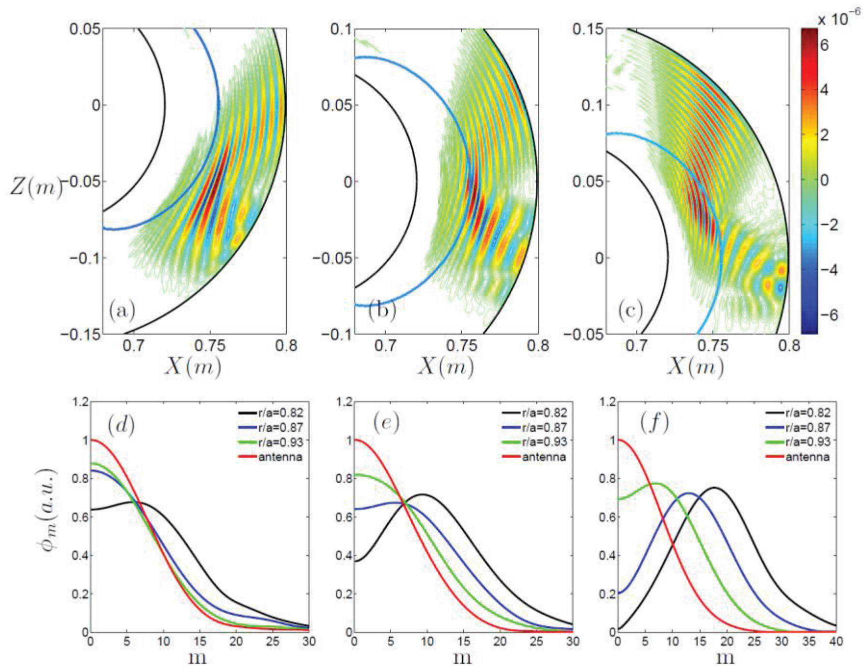

FIGURE 1. The slow wave is launched at (a) $\theta = 0$, (b) $\theta = 0.125\pi$ and (c) $\theta = 0.25\pi$, respectively. The theoretical mode conversion layer calculated by using fixed $n_{\|0} = n_t$ is shown as the line in panels (a), (b) and (c). Panels (d), (e) and (f) are the corresponding poloidal spectra of the slow wave-packets at various flux-surfaces.

PROPAGATION

In this section, we study the poloidal spectrum evolution of the LH wave-packet in a single pass. We launch the LH wave-packet at $\theta = 0$ position. The plasma is hot with an on-axis temperature $T_{e0} = 10.0keV$ and an on-axis density $n_{i0} = n_{e0} = 5.0 \times 10^{13} cm^{-3}$. The wave pattern structure and the poloidal mode spectrum at various flux-surfaces are shown in Fig. 2 (a) and (b), respectively. The central value of the poloidal spectrum of the LH wave-packet increases and the spectrum broadens with the wave penetrating towards the plasma center, which is due to the breaking of the poloidal symmetry and the wave diffractions.

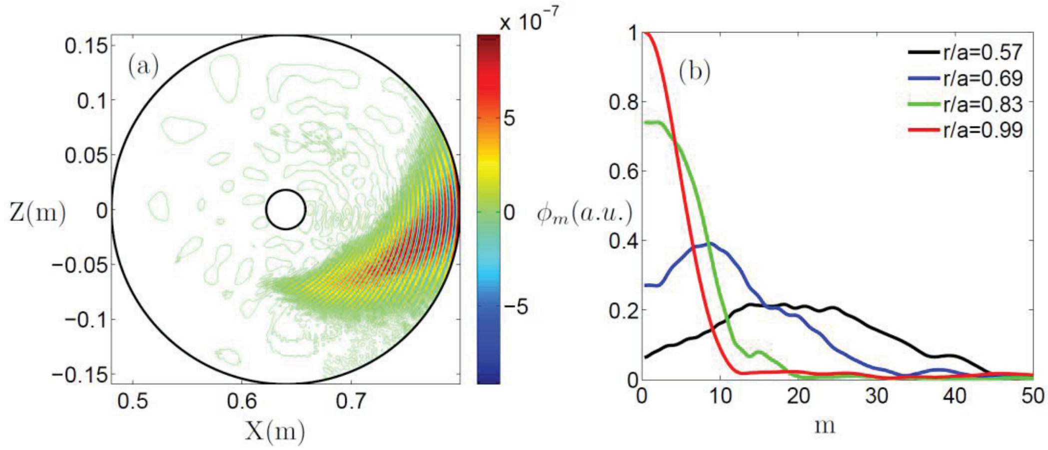

FIGURE 2. (a) Slow wave propagation in tokamak. (b) The poloidal spectrum of the wave-packet at different flux-surfaces.

CONCLUSIONS

Particle simulation approach is demonstrated as a new method for modelling LH wave in tokamak plasmas, which has advantages in studying nonlinear physics. GTC simulation shows the mode conversion between slow and fast waves if the accessibility condition is not satisfied, which agrees with the theory. Poloidal spectrum upshift and broadening effects in toroidal geometry are also observed in our simulation.

ACKNOWLEDGMENTS

This work was supported by China National Magnetic Confinement Fusion Science Program (Grant No. 2013GB111000), China Scholarship Council (Grant No. 201306010032) and US Department of Energy (DOE) SciDAC GSEP Program. This research used resources of the Oak Ridge Leadership Computing Facility at Oak Ridge National Laboratory (DOE Contract No. DE-AC05-00OR22725) and the National Energy Research Scientific Computing Center (DOE Contract No. DE-AC02-05CH11231).

REFERENCES

1. P. T. Bonoli, and E. Ott, Phys. Fluids **25**, 359 (1982).
2. J. C. Wright et al., Phys. Plasma **16**, 072502 (2009).
3. S. Shiraiwa et al., Phys. Plasma **17**, 056119 (2010).
4. Z. X. Lu, F. Zonca, and A. Cardinali, Phys. Plasma **20**, 032115 (2013).
5. G. M. Wallace et al., Phys. Plasma **17**, 082508 (2010).
6. P. T. Bonoli, and R. C. Englade **29**, 2937 (1986).
7. M. Porkolab et al., Phys. Fluids **20**, 2058 (1977).
8. R. Cesario, and A. Cardinali, Nucl. Fusion **29**, 1709 (1989).
9. F. Napoli et al., J. Phys.: Conf. Ser. **401**, 012016 (2012).
10. S. G. Baek et al., Plasma Phys. Control. Fusion **55**,052001 (2013).
11. S. G. Baek et al., Phys. Plasma **21**, 012506 (2014).
12. Z. Lin et al., Science **281**, 1835 (1998).
13. A. Kuley et al., Phys. Plasma **20**, 102515 (2013).
14. J. Bao et al., Plasma Phys. Control. Fusion **56**, 095020 (2014).
15. T. S. Hahm, W. W. Lee, and A. Brizard, Phys. Fluids **31**, 1940 (1988).
16. A. J. Brizard, and T. S. Hahm, Rev. Mod. Phys. **79**, 421(2007).
17. Y. Lin et al., Plasma Phys. Control. Fusion **47**, 657 (2005).